Master's Thesis

Highly Sensitive and Selectively Deposited Gold Nanoparticles on the Reduced Graphene Oxide for the SERS Application

Jeongyeop Lee

School of Molecular Science
(Chemistry)

Graduate School of UNIST

2016

Highly Sensitive and Selectively Deposited Gold Nanoparticles on the Reduced Graphene Oxide for the SERS Application

Jeongyeop Lee

School of Molecular Science
(Chemistry)

Graduate School of UNIST

Highly Sensitive and Selectively Deposited Gold Nanoparticles on the Reduced Graphene Oxide for the SERS Application

A dissertation
submitted to the Graduate School of UNIST
in partial fulfillment of the
requirements for the degree of
Master of Science

Jeongyeop Lee

12.02. 2015

Approved by

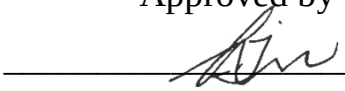

Advisor

Ji-Hyun Jang

Highly Sensitive and Selectively Deposited Gold Nanoparticles on the Reduced Graphene Oxide for the SERS Application

Jeongyeop Lee

This certifies that the dissertation of Jeongyeop Lee is approved.

12. 02. 2015

signature

Advisor: Ji-Hyun Jang

signature

Sang Hoon Joo

signature

Hyunhyub Ko

Abstract

Surface enhanced Raman scattering (SERS) is the enhancement of the Raman signal by several orders of magnitude via the electromagnetic enhancement or the chemical enhancement of metal nanostructures. In addition, graphene also has a Raman enhancement by its novel property that is referred to graphene enhanced Raman scattering (GERS). In this, we combined electromagnetic enhancement of the gold nanoparticles which has a selectivity onto the sp2 carbon surface and the GERS effect of patterned reduced graphene oxide (prGO) for the highly sensitive and stable SERS platform. Our SERS substrate can be applied to the diagnostic SERS device and also enables the selective and dense attachment of metal nanoparticles on the graphene surface.

Contents

List of Figures

List of Tables

Chapter 1. Introduction of Surface-Enhanced Raman Scattering (SERS)

1.1 Raman Scattering and SERS

Raman scattering is the inelastic scattering of a photon. It has been discovered by C. V. Raman. When photons are scattered from the surface of molecules or atoms, most photons are showing elastic scattering (Rayleigh scattering) which scattered photons maintain same amount of energy between irradiation/radiation. At the same time, a quite small portion of the photons are scattered with slightly reduced or enhanced energy that calls Raman scattering. Usually, the frequency of scattered photons is lower than the incident photons.

Raman spectroscopy is exploited for the precise and robust identification of common molecules. Although Raman spectroscopy is limited by low sensitivity, SERS can provide the signal intensity of the molecules enhanced by several magnitudes. Since the discovery of the greatly enhanced Raman signals of the molecules on a rough metallic surface, SERS has been proposed as an efficient detection tool for a variety of ultrasensitive chemical and biological sensing applications. However, due to the rather weak and unstable signal of enhanced Raman scattering from the substrate, SERS studies have still been a problem and an answer for ongoing research works in sensing areas.

The intensity of SERS signal is based on the enhancement from two mechanism: electromagnetic mechanism (EM) or the chemical mechanism (CM).

EM is based on the following statements

- Local electric fields of the metallic nanostructures caused by surface plasmon resonance (SPR)
- This enhancement occurs at the sharp metal or the nanosize gap structure
- EM is the dominating enhancement mechanism than CM

Because of an enhancement in the electric field provided by the surface, the increment in intensity of the SERS signal for molecules on metal surface occurs. While the surface has been excited by the incident light, the SPR enhances the field enhancement which is greatest when the plasmon frequency is in resonance with the excitation. It has been reported that the SPR of two or more metal nanoparticles can create an area with a huge Raman increment, called a local ‘hot spot’, which contributes to a strong SERS effect with a theoretical enhancement factor of 10^3-10^{10}.

The CM is not fully understood the magnitude of the signal intensity observed in many areas. For the various molecules in interaction with a metal, charge transfer resonance including a resonance Raman

effect engaged with chemical interactions between the molecules and the metal surfaces. If the potential is scanned at a fixed laser frequency, or the potential, wide range of resonances are observed. The electronic states which is appeared from chemisorption supported as resonant states of Raman scattering.

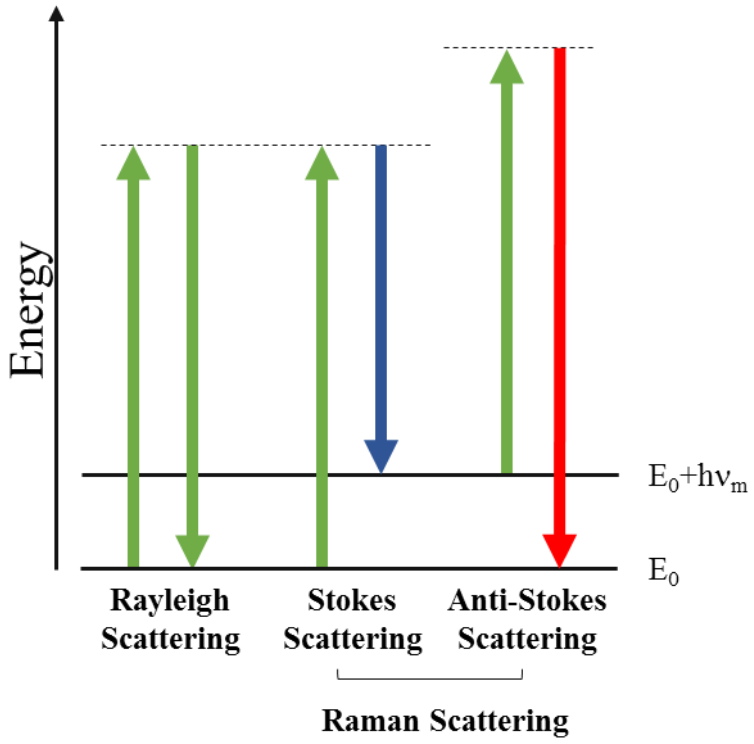

Figure 1.1 Energy diagram of light scattering

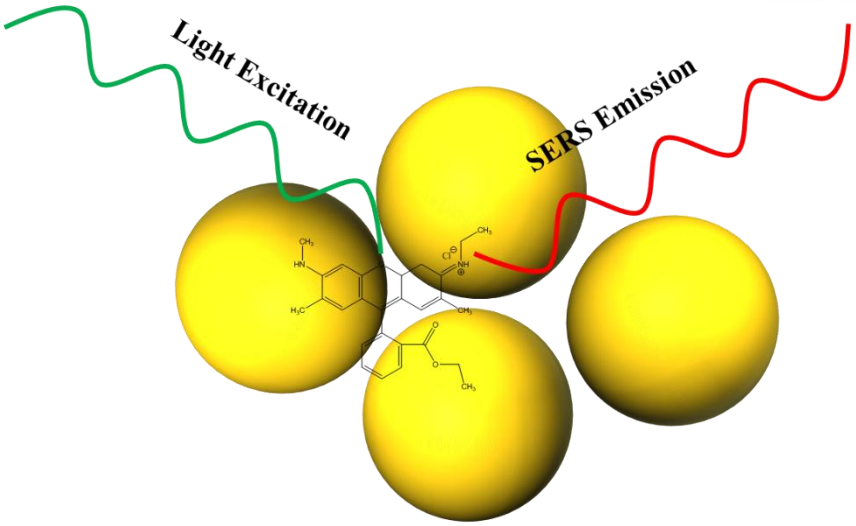

Figure 1.2 Schematic illustration of SERS

1.2 Graphene-Enhanced Raman Scattering (GERS)

Graphene, a monolayer carbon atoms in a sp^2-bonded honeycomb lattice, was discovered to be an active substrate with excellent Raman enhancement of adsorbed molecules, a phenomenon known as graphene enhanced Raman scattering (GERS). Further, graphene, known as a fluorescence quencher, has advantage in resolving the problem related with the rough fluorescence background from the laser-assisted excitation of dyes. Because of the optical absorption of graphene and THz frequency region of the graphene plasmon, the GERS was considered to be only from the CM enhancement, with absence of EM contribution. The GERS is growing interest of many researches due to not only its unique chemical and electrical performance but also its unexplained mechanism at the Raman enhancement.

1.3 References

1. Fleischmann, M.; Hendra, P. J.; Mcquilla.Aj, Raman-Spectra of Pyridine Adsorbed at a Silver Electrode. *Chem. Phys. Lett.* **1974,** *26* (2), 163-166.
2. Albrecht, M. G.; Creighton, J. A., Anomalously Intense Raman-Spectra of Pyridine at a Silver Electrode. *J. Am. Chem. Soc.* **1977,** *99* (15), 5215-5217.
3. Jeanmaire, D. L.; Van Duyne, R. P., Surface raman spectroelectrochemistry. *J. Electroanal. Chem. and Interfacial Electrochem.* **1977,** *84* (1), 1-20.
4. Ko, H.; Tsukruk, V. V., Nanoparticle-Decorated Nanocanals for Surface-Enhanced Raman Scattering. *Small* **2008,** *4* (11), 1980-1984.
5. Freudiger, C. W.; Min, W.; Saar, B. G.; Lu, S.; Holtom, G. R.; He, C.; Tsai, J. C.; Kang, J. X.; Xie, X. S., Label-Free Biomedical Imaging with High Sensitivity by Stimulated Raman Scattering Microscopy. *Science* **2008,** *322* (5909), 1857-1861.
6. Kundu, J.; Levin, C. S.; Halas, N. J., Real-time monitoring of lipid transfer between vesicles and hybrid bilayer on Au nanoshells using surface enhanced Raman scattering (SERS). *Nanoscale* **2009,** *1* (1), 114-117.
7. Ren, W.; Fang, Y. X.; Wang, E. K., A Binary Functional Substrate for Enrichment and Ultrasensitive SERS Spectroscopic Detection of Folic Acid Using Graphene Oxide/Ag Nanoparticle Hybrids. *ACS Nano* **2011,** *5* (8), 6425-6433.
8. Reed, J. C.; Zhu, H.; Zhu, A. Y.; Li, C.; Cubukcu, E., Graphene-Enabled Silver Nanoantenna Sensors. *Nano Lett.* **2012,** *12* (8), 4090-4094.
9. Peng, P.; Huang, H.; Hu, A. M.; Gerlich, A. P.; Zhou, Y. N., Functionalization of silver nanowire surfaces with copper oxide for surface-enhanced Raman spectroscopic bio-sensing. *J. Mater. Chem.* **2012,** *22* (31), 15495-15499.
10. Lin, D.; Qin, T.; Wang, Y.; Sun, X.; Chen, L., Graphene Oxide Wrapped SERS Tags: Multifunctional Platforms toward Optical Labeling, Photothermal Ablation of Bacteria, and the Monitoring of Killing Effect. *ACS Appl. Mater. Inter.* **2014,** *6* (2), 1320-1329.
11. Ling, X.; Xie, L.; Fang, Y.; Xu, H.; Zhang, H.; Kong, J.; Dresselhaus, M. S.; Zhang, J.; Liu, Z., Can Graphene be used as a Substrate for Raman Enhancement? *Nano Lett.* **2010,** *10* (2), 553-561.
12. Schedin, F.; Lidorikis, E.; Lombardo, A.; Kravets, V. G.; Geim, A. K.; Grigorenko, A. N.; Novoselov, K. S.; Ferrari, A. C., Surface-Enhanced Raman Spectroscopy of Graphene. *ACS Nano* **2010,** *4* (10), 5617-5626.
13. Ling, X.; Zhang, J., First-layer effect in graphene-enhanced Raman scattering. *Small* **2010,** *6* (18), 2020-5.
14. Xu, W. G.; Mao, N. N.; Zhang, J., Graphene: A Platform for Surface-Enhanced Raman Spectroscopy. *Small* **2013,** *9* (8), 1206-1224.
15. Ling, X.; Huang, S.; Deng, S.; Mao, N.; Kong, J.; Dresselhaus, M. S.; Zhang, J., Lighting Up the Raman Signal of Molecules in the Vicinity of Graphene Related Materials. *Acc. Chem. Res.* **2015**.
16. Huh, S.; Park, J.; Kim, Y. S.; Kim, K. S.; Hong, B. H.; Nam, J. M., UV/Ozone-Oxidized Large-Scale Graphene Platform with Large Chemical Enhancement in Surface-Enhanced Raman Scattering. *ACS Nano* **2011,** *5* (12), 9799-9806.

Chapter 2. Synthesis and Characterization of Dendrimer Encapsulated Gold Nanoparticles (Au-Den) with Optimum Size

2.1. Introduction

The dendrimer is the huge organic molecules which has many functional groups at the end of branches. In this work, we used amine functionmalized dendrimer (PAMAM-G4) which has 32 amine groups at the ends and many amide groups at the each separating branches. Normally, PAMAM-G4 was used as the endo-type encapsulation of Au nanoparticles with the diameter ranged about 3-5 nm. But we modified the preparation method and propagation mechanism so that grow up the average size to 35 nm. We measured prepared Au-Den using SEM, TEM, and Raman spectroscopy and then analyze the effect of dendrimer at the gold nanoparticle surface.

2.2 Experimental Procedures

2.2.1 Synthesis of Au-Den

0.04 μmol of PAMAM-G4 was dissolved in 18.76 ml of water and 8 μmol of $HAuCl_4$ in 200 μL of water. These two solutions are mixed and stirred less than a minute to homogenize Au precursor. Then, prepared solution was heated under 100 ^oC for 60 min. The 10 μL of solution was dropped on the SiO_2/Si surface and naturally dried for the characterization.

2.2.2 Characterization

The prepared structure was analyzed by field-emission scanning electron microscopy (FE-SEM, FEI Nano 230) and atomic force microscopy (AFM, Veeco). Prepared Au-Den was characterized by FT-IR spectroscopy, UV-Vis spectroscopy, PL measurement, transmission electron microscopy (TEM, JEOL TEM 2100). To confirm the SERS performance of the prepared substrate, combined AFM-Raman microscopy (WITec) was used to confirm the signal enhancement of the dye. Aqueous R6G was prepared to a concentration of 1 mM to obtain a stock solution and then with the adjusted amount of water. The substrate was dipped into the dye solution and kept for 60 min to stabilize the deposition equivalently. After adsorption, the substrate was rinsed by DI water. For the general Raman measurement, the 532 nm wavelength of laser was used with the power adjustment to 0.2 mW and the

integration time was set to be 30s.

2.3 Results and Discussion

The Au-Den was prepared by simple one-step preparation method. The deposited Au-Den on the SiO_2/Si substrate. The illustration of Figure 2.1 presents the formation of Au-Den nanocluster.

The fabrication process of Au-Den is displayed in Figure 2.1. The illustration shows the simple preparation method of Au-Den as reported by Crooks et al. with slight modification in the method of reducing Au precursors. We applied thermal heating rather than chemical reducing in order to achieve the optimized size of nanoparticles for the strong SERS signal enhancement. Even though PAMAM is known to make 1-2 nm size of endo-type nanoparticles by the reducing reagents, we were able to create about 35 nm dendrimer-stabilized Au nanoparticles by thermal reduction. Figure 2.2 supports that our strategy was successfully achieved and shows aggregated Au particles on the bare SiO2 substrate with an average diameter of 35 nm, which is stabilized by 1-2 nm thick dendrimers. It has been reported that the charge transfer for the Raman enhancement between dye and Au NPs with the distance less than 5 nm is not interrupted and the dendrimer moreover has the capability to contain small molecules such as dyes or drugs in the form of the molecular container. Therefore, our Au-Den has a SERS active morphology such that aggregated Au NP is wrapped by a 1-2 nm thick dendrimer in diameter with percolated dye molecules in the cage of the dendrimer keeping the distance between dye molecules and Au NPs less than 5 nm. The UV-Vis spectra of Au-Den aqueous solution (Figure 2.3) indicates the clear formation of Au-Den. The single peak of Au-Den with maximum absorption at the position of 525 nm implies that the spherical particle formation of Au-Den with the rough size about 30~40 nm. We measured SERS performance of Au-Den on the SiO_2/Si substrate. The representative peak at the 1369 cm^{-1} is the significant to compare the intensity with other conditions or substrates. The intensity of that peak was about 2 K at the integration time of 30 s. It is similar with the normally prepared gold nanoparticle (AuNP) with the absence of dendrimer so it indicates that the dendrimer does not interrupt the SERS activity at the Au-Den surface.

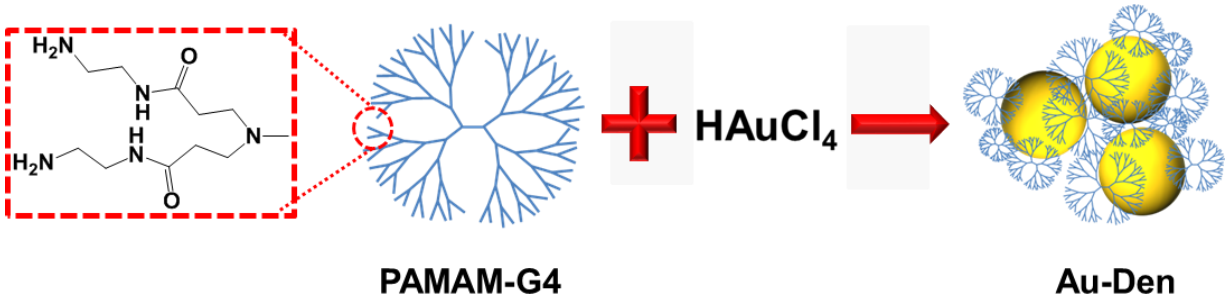

Figure 2.1 Schematic illustratiuon of Au-Den nanocluster.

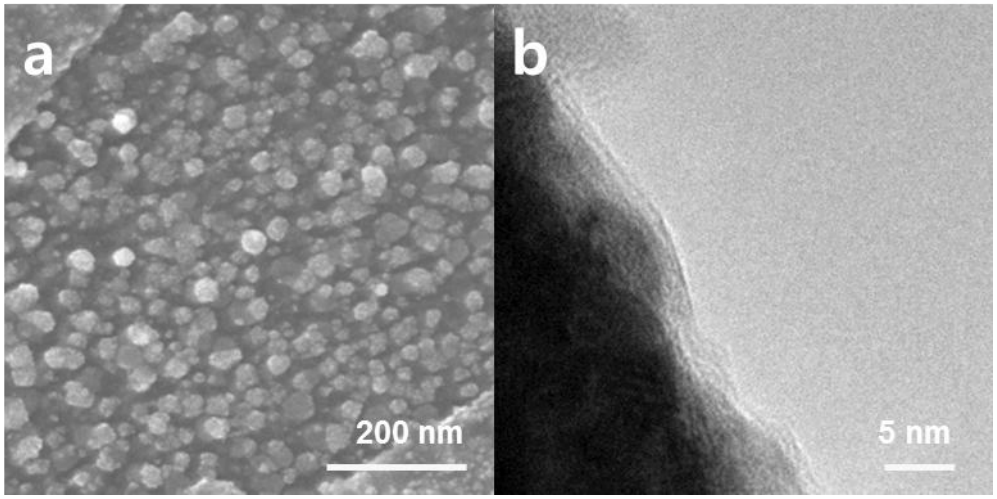

Figure 2.2 SEM (a) and TEM (b) image of Au-Den nanocluster.

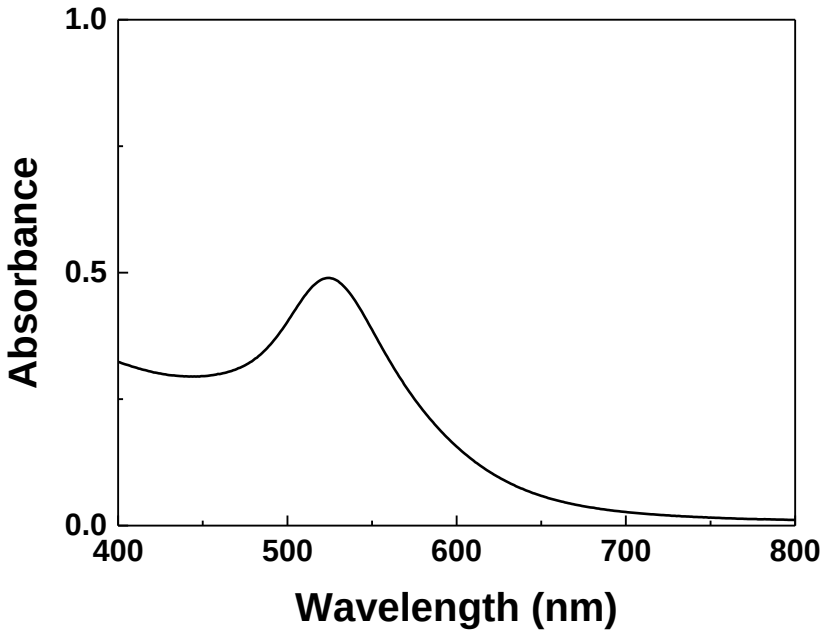

Figure 2.3 UV-Vis spectra of Au-Den solution.

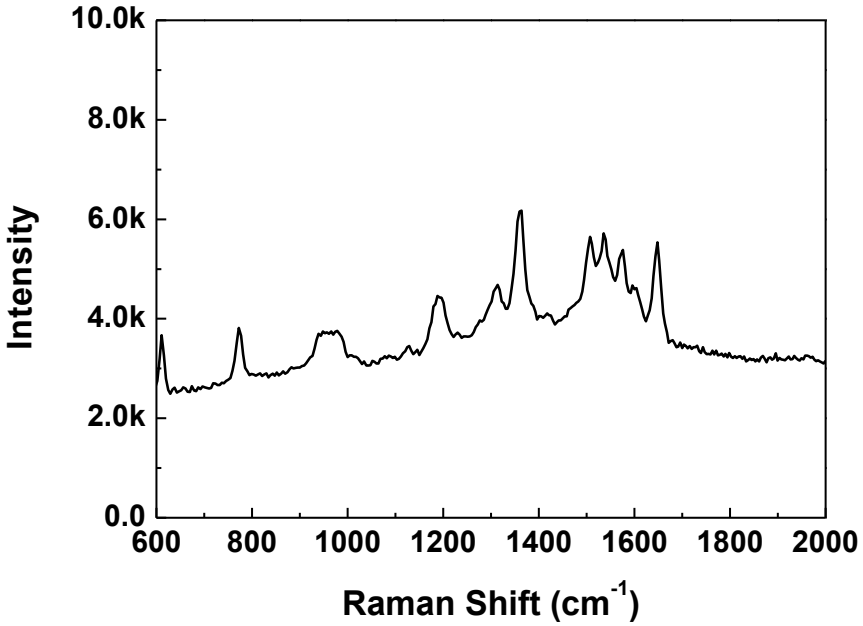

Figure 2.4 SERS of Au-Den on the SiO_2/Si substrate.

2.4 Conclusion

In summary, we have presented that the preparation of the Au-Den by using dendrimer as the stabilizing and SERS supporting agent via the simple one step method. The prepared particle shows the diameter of 35 nm with the perfect spherical shape. The SERS signal was shown as well prepared Au clusters but encapsulated dendrimer does not interrupt the SERS performance. This results totally indicates that our first goals was successfully achieved and then we can carefully accomplish the application of Au-Den to the reduced graphene oxide surface.

2.5 References

1. Fleischmann, M.; Hendra, P. J.; Mcquilla.Aj, Raman-Spectra of Pyridine Adsorbed at a Silver Electrode. *Chem. Phys. Lett.* **1974,** *26* (2), 163-166.
2. Albrecht, M. G.; Creighton, J. A., Anomalously Intense Raman-Spectra of Pyridine at a Silver Electrode. *J. Am. Chem. Soc.* **1977,** *99* (15), 5215-5217.
3. Jeanmaire, D. L.; Van Duyne, R. P., Surface raman spectroelectrochemistry. *J. Electroanal. Chem. and Interfacial Electrochem.* **1977,** *84* (1), 1-20.
4. Ko, H.; Tsukruk, V. V., Nanoparticle-Decorated Nanocanals for Surface-Enhanced Raman Scattering. *Small* **2008,** *4* (11), 1980-1984.
5. Freudiger, C. W.; Min, W.; Saar, B. G.; Lu, S.; Holtom, G. R.; He, C.; Tsai, J. C.; Kang, J. X.; Xie, X. S., Label-Free Biomedical Imaging with High Sensitivity by Stimulated Raman Scattering Microscopy. *Science* **2008,** *322* (5909), 1857-1861.
6. Kundu, J.; Levin, C. S.; Halas, N. J., Real-time monitoring of lipid transfer between vesicles and hybrid bilayer on Au nanoshells using surface enhanced Raman scattering (SERS). *Nanoscale* **2009,** *1* (1), 114-117.
7. Lee, J.; Hua, B.; Park, S.; Ha, M.; Lee, Y.; Fan, Z.; Ko, H., Tailoring surface plasmons of high-density gold nanostar assemblies on metal films for surface-enhanced Raman spectroscopy. *Nanoscale* **2014,** *6* (1), 616-23.
8. Kim, Y. G.; Oh, S. K.; Crooks, R. M., Preparation and characterization of 1-2 nm dendrimer-encapsulated gold nanoparticles having very narrow size distributions. *Chem. Mater.* **2004,** *16* (1), 167-172.
9. Fu, Q.; Zhan, Z.; Dou, J.; Zheng, X.; Xu, R.; Wu, M.; Lei, Y., Highly Reproducible and Sensitive SERS Substrates with Ag Inter-Nanoparticle Gaps of 5 nm Fabricated by Ultrathin Aluminum Mask Technique. *ACS. Appl. Mater. Inter.* **2015,** *7* (24), 13322-8.
10. Jansen, J. F. G. A.; Debrabandervandenberg, E. M. M.; Meijer, E. W., Encapsulation of Guest Molecules into a Dendritic Box. *Science* **1994,** *266* (5188), 1226-1229.
11. Herrero, M. A.; Guerra, J.; Myers, V. S.; Gomez, M. V.; Crooks, R. M.; Prato, M., Gold Dendrimer Encapsulated Nanoparticles as Labeling Agents for Multiwalled Carbon Nanotubes. *Acs Nano* **2010,** *4* (2), 905-912.
12. Kim, J. M.; Kim, J.; Kim, J., Covalent decoration of graphene oxide with dendrimer-encapsulated nanoparticles for universal attachment of multiple nanoparticles on chemically converted graphene. *Chem. Commun.* **2012,** *48* (74), 9233-5.
13. Suzuki, M.; Niidome, Y.; Kuwahara, Y.; Terasaki, N.; Inoue, K.; Yamada, S., Surface-enhanced nonresonance Raman scattering from size- and morphology-controlled gold nanoparticle films. *J Phys Chem B* **2004,** *108* (31), 11660-11665.
14. Mir-Simon, B.; Reche-Perez, I.; Guerrini, L.; Pazos-Perez, N.; Alvarez-Puebla, R. A., Universal One-Pot and Scalable Synthesis of SERS Encoded Nanoparticles. *Chem. Mater.* **2015,** *27* (3), 950-958.

Chapter 3. Selectively Deposited Gold Nanoparticles on the Reduced Graphene Oxide for the High Sensitivity and Stability

3.1 Introduction

In this research, we report dendrimer encapsulated AuNPs (Au-Den) deposited on a rGO substrate as an efficient SERS platform that allows the strongly enhanced and highly stable Raman signal of probe molecules by exploiting the affinity of dendrimer on rGO. The essential advantages of coupling of AuNPs with a dendrimer can be described as follows: i) Au-Den has a dense packing ability of Au NPs on the rGO substrate due to a strong affinity on the surface of sp^2 carbon materials, which leads to a greatly enhanced SERS signal. Furthermore, the much stronger affinity of Au-Den with the graphitic compounds than other materials finally allows selective deposition of Au-Den on the patterned graphene surface. The directly patternable graphene/metal NPs substrate with enhanced SERS properties may expands the applications of SERS substrates to many delicate electrical devices and diagnostics. ii) SERS enhancement of dye molecules on the Au-Den/rGO remained almost unchanged for one hour's duration of irradiation and more than a year due to the highly stable surface protection of Au NPs by the dendrimer moiety in Au-Den. This is very promising considering that previous studies showed limited enhancement of Raman peaks, with either fluctuation or rapid damping of the signal intensity due to surface activation of metal NPs induced by laser irradiation during the measurement.

3.2 Experimental Procedures

3.2.1 Preparation of Au-Den/prGO

To synthesize graphene oxide, we used a modified Hummer's method. 1 mg/ml of GO solution was spin-coated on a Si wafer (200 nm SiO2) after being treated with a piranha solution. The GO-coated wafer was dried at 80 ^{o}C for 6 hrs. To reduce the pre-treated GO substrate to rGO, the substrate was annealed at 1000 ^{o}C for 30 min under an Ar/H_2 atmosphere. The prGO was prepared via photolithography. A 1.4 μm thick positive tone photoresist (AZ5214) was spin-coated onto the rGO substrate and soft baked at 105 ^{o}C for 1 min. The soft baked films were exposed to an I-line source (Midas/MDA-6000 DUV, KR; wavelength: 365 nm; 9.5 mW/cm2) through a photo mask and post-baked at 110 ^{o}C for 1 min. Subsequently, the patterns were developed by MIF-300 solution for 30 sec.

The patterns of the photoresist film were transferred to the rGO layer by oxygen reactive ion etching (SHE-4D-20, Sam-Han Development). The oxygen gas flow rate, RF power, and pressure in the chamber were 50 sccm, 20 W, and 300 mTorr, respectively. The remaining photoresist films were removed by immersing the films in acetone for 1 min. For the assembly of Au-Den on the prGO substrate, 80 µL of a PAMAM-G4 solution in MeOH (0.18 mM) and 250 µL of a $HAuCl_4$ (10 mM) aqueous solution were added to 19.65 ml of DI water and stirred for less than a minute to homogenize the Au precursors. The as prepared prGO/SiO2/Si was then immersed into the precursor solution and heated at 100 ^oC for 60 min followed by washing with DI water. This procedure was repeated 3 times. To control the size of Au-Den (10 nm), a diluted $HAuCl_4$ solution (50 µL) was used.

3.2.2 Characterization

The prepared structure was analyzed by field-emission scanning electron microscopy (FE-SEM, FEI Nano 230) and atomic force microscopy (AFM, Veeco). Prepared Au-Den was characterized by FT-IR spectroscopy, UV-Vis spectroscopy, PL measurement, transmission electron microscopy (TEM, JEOL TEM 2100). To confirm the SERS performance of the prepared substrate, combined AFM-Raman microscopy (WITec) was used to confirm the signal enhancement of the dye. Aqueous R6G was prepared to a concentration of 1 mM to obtain a stock solution and then with the adjusted amount of water. The substrate was dipped into the dye solution and kept for 60 min to stabilize the deposition equivalently. After adsorption, the substrate was rinsed by DI water. For the general Raman measurement, the 532 nm wavelength of laser was used with the power adjustment to 0.2 mW and the integration time was set to be 10s.

3.3 Results and Discussion

The GO was prepared by Hummer's method was coated on the amino silane-treated SiO_2/Si substrate followed by subsequent reduction under an Ar/H_2 atmosphere. Patterned rGO (prGO) was created by photolithography after removing the positive photoresists. *In-situ* selective deposition of Au-Den on prGO was then achieved during thermal reduction of the Au^{3+} ions, and Au^0 atoms were stabilized by PAMAM-G4 by forming Au-Den as shown in Figure 3.1. Due to the favorable encapsulation of R6G dyes in dendrimer, the gap between two or more nanoparticle was kept less than 5 nm which is optimized for the strong SERS signal was able to be maximized while retaining the resistance to the oxidation of metal NPs in an ambient condition.

Figure 3.2 describes the formation of the highly selective and densely packed Au-Den on the prGO substrate due to the strong noncovalent binding between RGO and Au capping dendrimers. We prepared a few-layer sheets of prGO (AFM result of rGO sheets are in Figure 3.3) with holes having a diameter of 5 μm in a square lattice pattern with a center to center distance of 5 μm on the SiO_2/Si substrate, as shown in Figure 3.3a. As can be seen in Figure 3.3b, Au-Den is uniformly deposited only on the region of prGO, indicating highly selective deposition which confirms much stronger binding of Au-Den on prGO compared to on the SiO2 substrate. AFM images in Figures 3.3c and 3.3d clearly demonstrate the uniform and selectively deposited morphology of Au-Den on the prGO region. The physical binding between the dendrimer and rGO is supported by the charge transfer-induced strong van der Waals interactions between the amine groups in the dendrimer and the sp^2 hybridized carbons in rGO, eventually allowing for dense packing of Au-Den on rGO. Note that the SERS enhancement from AuNPs is increased by local 'hot spots' generally achieved by aggregation induced nano-gaps among two or more AuNPs. Therefore, the densely packed morphology of Au-Den is believed to lead to the strong SERS signal of R6G on the Au-Den/prGO. Further, the direct and simple patterning of AuNPs with enhanced SERS properties as we have presented may have potential value in many electrical devices and sensing applications which need specific signal recognition.

The detailed formation of Au-Den on the rGO surface was shown in Figure 3.4. Figure 3.4a and 3.4b shows the before/after rGO deposition on the grid. SEM image of Au-Den/rGO in Figure 3.4c supports our 35 nm size of Au-Den formation on the rGO surface. The TEM image of 3.4d also shows the encapsulation of dendrimer at the Au surface.

In order to confirm the successful deposition of Au-Den on the rGO surface, XPS spectra of the Au-Den/rGO film were obtained. We prepared the sample by 3 times of successive deposition of Au-Den on rGO and subsequent washing of the substrate to remove excess Au ions and PAMAM-G4 molecules. After the Au-Den deposition, the peaks of carbonate groups at the position of 287.5 eV in C 1s (Figure 3.5a) and 530.5 eV in O 1s (Figure 3.5b), N 1s (Figure 3.5c) binding peaks at the position of 399.5 eV and 402 eV from amide and the amine groups, and a Au 4f peak at 83.6 eV and 87.3 eV (Figure 3.5d) appeared, which clearly confirms the successful binding of Au-Den on the rGO substrate.

Figure 3.6 compares the Raman peaks of Rhodamine 6G (R6G) dye molecules on the rGO and Au-Den/rGO substrate. The substrates were dipped into a 10^{-6} M R6G solution, which is the common SERS reporter and concentration, and washed thoroughly to remove residual R6G molecules. When GERS was supported, the Raman peaks of R6G on the rGO substrate were clearly visible, as shown in Figure 3.6 (in black). This is in accordance with an enhancement factor of GERS in a range of $10\text{-}10^4$. Besides, as expected, we observed the fluorescent background of R6G dye molecules with a maximum fluorescent wavelength at 524 nm has been successfully quenched under the 532 nm laser

irradiation, though the signal intensity is much lower than that of an EM supported substrate. After Au-Den deposition on rGO (in red), the Raman signal of R6G meaningfully increased, indicating the creation of a highly sensitive and efficient SERS substrate supported by both EM and CM.

In order to demonstrate that our substrate works with extremely high sensitivity as well as selectivity, we performed Raman spectral mapping of the peak at 1370 cm^{-1} in Figures 3.7a and 3.7d. The bright region in the Raman spectral mapping image in Figure 5a represents the presence of AuNPs spread irregularly on the SiO_2/Si substrate. On the contrary, Au-Den/prGO presented a clear bright Raman spectral mapping image that projects the pattern shape of the bottom prGO, indicating highly selective deposition of Au-Den onto the prGO substrate (Figure 3.7d). When we compared the peak intensity of R6G molecules at 1370 cm^{-1} between the bright region and dark region in Figure 3.7d, $I_{Au\text{-}Den/prGO}/I_{Au\text{-}Den}$ was about 80, indicating that the Au-Den/prGO supported by graphene is a powerful SERS reporter and that it has potential for real sensing applications on devices. Figure 3.7b and 3.7e compares the Raman signal of the R6G dyes on the AuNPs/SiO_2 and the Au-Den/prGO/SiO_2 substrates to verify the role of graphene and the dendrimer in our system. AuNPs showed an intensity of 950 at 1370 cm^{-1} (Figure 3.7b) whereas Au-Den/prGO allows an intensity of about 10 k at 1370 cm^{-1} (Figure 3.7e), which is an order higher intense Raman signal of dye. This reveals the synergetic effects of the EM of Au-Den and the CM of prGO in our SERS platform.: Unusually remarkable enhancement of the Raman signal on the Au-Den/rGO substrate compared to on other AuNP/graphene substrates suggests there are some other critical factors such as charge transfer-induced strong interactions rather than a simple combinatory effect of the EM caused by Au-Den and the CM by rGO. We attributed this to a significant impact of the population of Au clusters on the substrate on SERS. The population of Au-Den particles on the SiO_2 substrate counted from the SEM image was about 110 per 1 μm^2, whereas that of AuNP was 30/μm^2. The dense packing of Au-Den on the reduced graphene oxide was achieved by the strong affinity between Au-Den and the graphene surface as confirmed previously. The contrast in SEM images (Figure 3.8), due to the deposition of Au-Den on barely coated rGO, further implies the possibility of any arbitrary pattern formation induced by the selective binding. It clearly demonstrates that rGO not only amplifies the existing Raman signal intensity of R6G but also wisely guides much more Au-Dens on the specific position of the substrate. In addition, the guiding characteristic of rGO was not affected by the size of the Au-Den as shown in Figure 3.9, which opens the possibility of the AuNP/graphene hybrid materials with the optimized size for the explicit application area.

To quantize the enhancement effect of our SERS substrate, the enhancement factor (EF) was obtained by the following equation using the NRS of R6G as a reference.

$$EF = \frac{N_{Ref} \times I_{SERS} \times \tau_{Ref} \times P_{Ref}}{N_{SERS} \times I_{Ref} \times \tau_{SERS} \times P_{SERS}} \quad \textbf{(1)}$$

In eq. (1), N_{Ref} and N_{SERS} are the number of R6G molecules adsorbed onto the reference and the SERS substrates, respectively. I_{Ref} and I_{SERS} are the intensity of the corresponding normal Raman and the SERS peaks. First, for the quantitative analysis of the R6G molecules on the substrate, we dropped proper concentration of R6G solution on the 10 x 10 mm^2 area of both the NRS and SERS substrate with subsequent washing and enough drying time. Then, we obtained the NRS results from a 20 mW laser with 10 s of integration time and SERS was carried out under 0.2 mW laser power for the same integration time. Using this process, we could calibrate the effect of the laser power and the integration time. In total, R6G on Au-Den/prGO showed an EF value of 2.5 x 10^8 (Detailed information on calculation is described in table 3.1). The most important achievement by coupling Au-Den onto the SERS substrate is the stability of the Raman signal. Figure 3.7c and 3.7f displayed the Raman signal retention of dyes on the AuNP/SiO_2 and Au-Den/rGO/SiO_2 substrate at the peak of 1370 cm^{-1}. 95 % of the Raman signal of dyes on Au-Den/rGO remains for more than 1 year, whereas the signal on AuNP/SiO_2 was apparently reduced to half of initial after 2 months. Further, we tested the stability of the signal intensity during the laser irradiation. Figure 3.7g confirmed substantially stable performance of the Au-Den/prGO substrate, where ~93 % of the Raman signal was retained for 1 hour of laser exposure. The highly stable signal of dyes can be attributed to the stabilization of Au capped by dendrimer while keeping the same intensity Raman signal as the one without dendrimer having direct contact between dyes and Au NPs, demonstrating the extraordinary robustness of the SERS substrate realized by our suggested system. For a further quantitative analysis of R6G, the loading amount of dyes was varied by controlling the concentration of the R6G solution dropped onto the substrate, as shown in Figure 3.7h. The results confirmed that our substrate can detect a few hundred molecules in the area of circle of Au-Den/rGO substrate with a diameter of 1 μm.

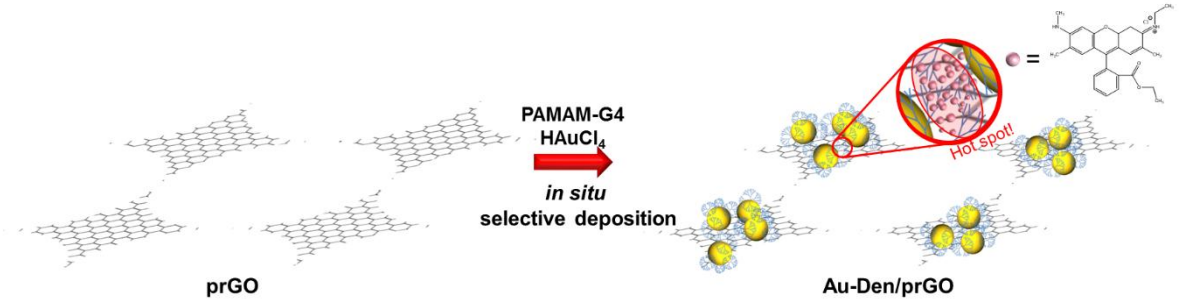

Figure 3.1 A schematic of in-situ selective deposition of Au-Den on patterned rGO.

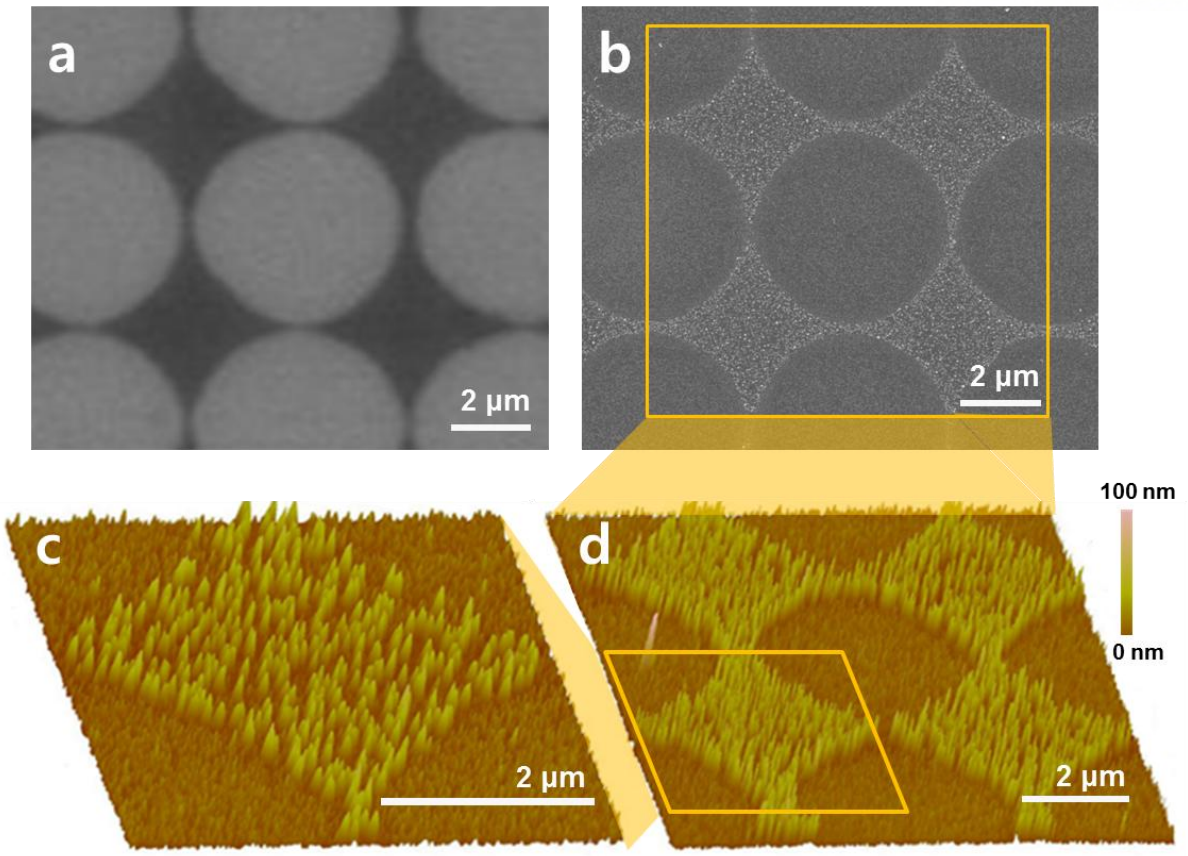

Figure 3.2 SEM image of patterned (a) rGO, (b) Au-Den/prGO, and (c, d) 3D-AFM images of Au-Den/prGO.

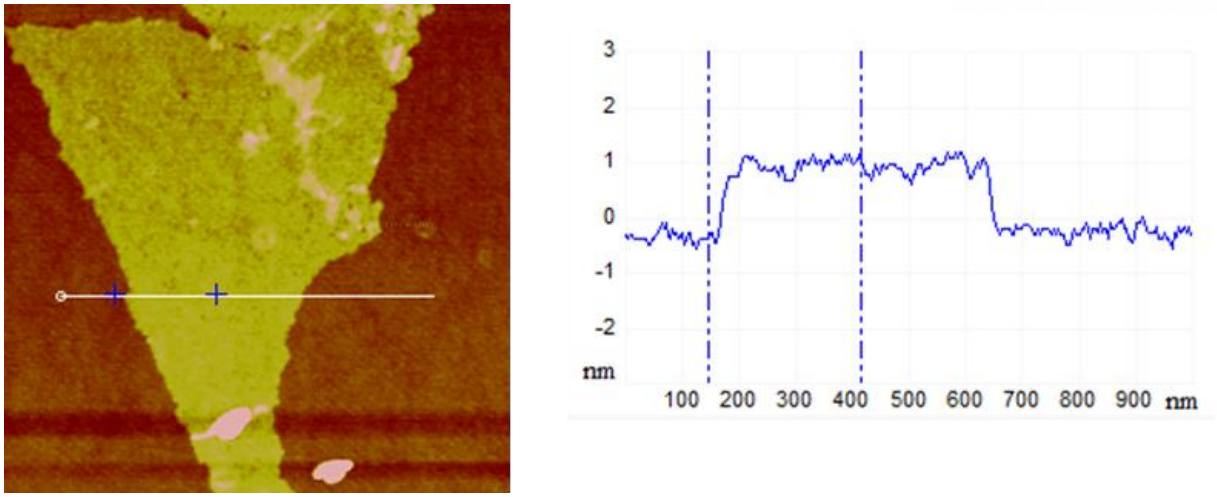

Figure 3.3 AFM image of rGO sheet on Si wafer

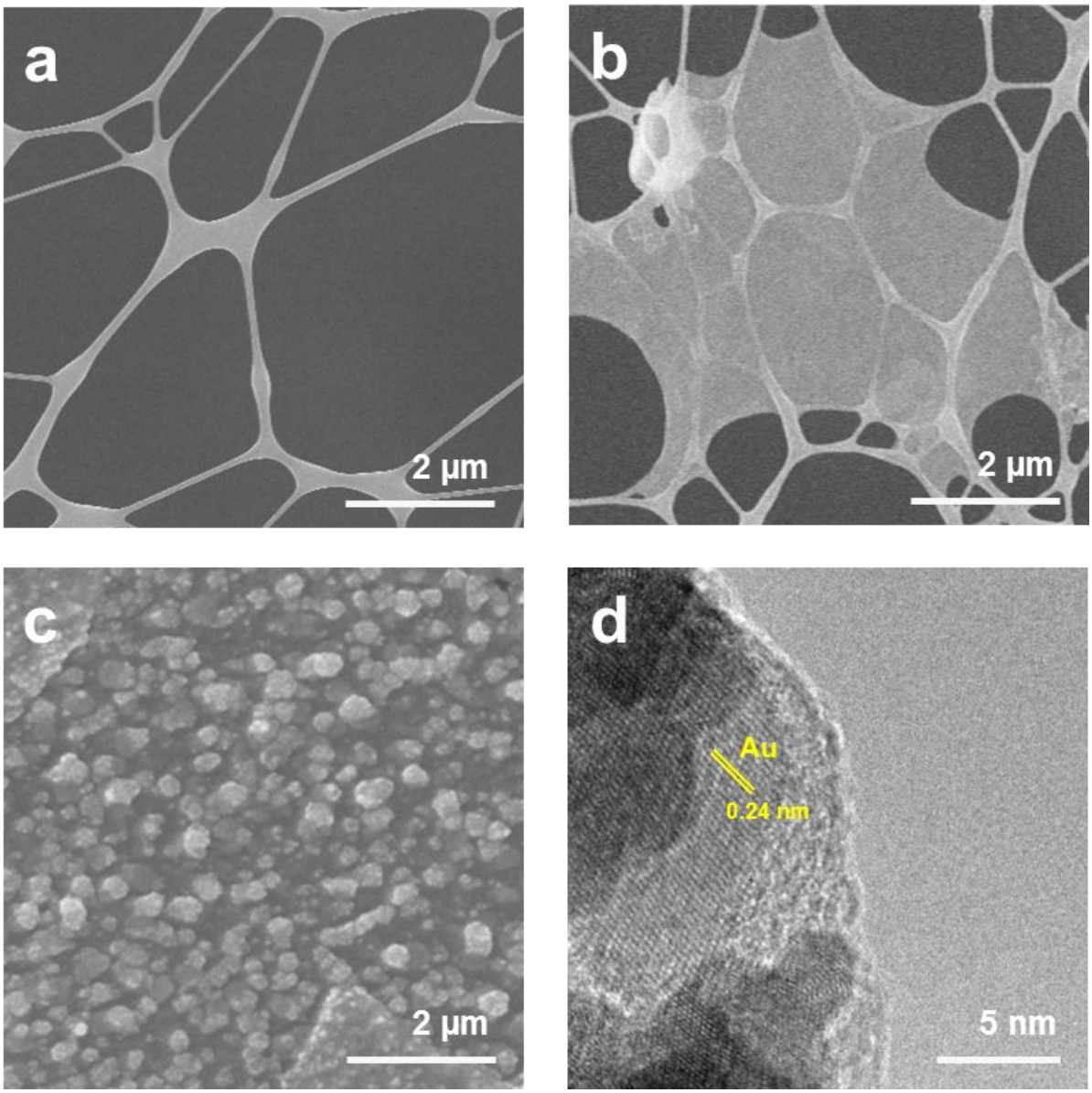

Figure 3.4 SEM and TEM image of various samples (a: bare lacey grid, b: rGO with lacey grid, c: Au-Den on the rGO on lacey grid, d: TEM image of Au-Den on rGO, amorphous layer is PAMAM dendrimer)

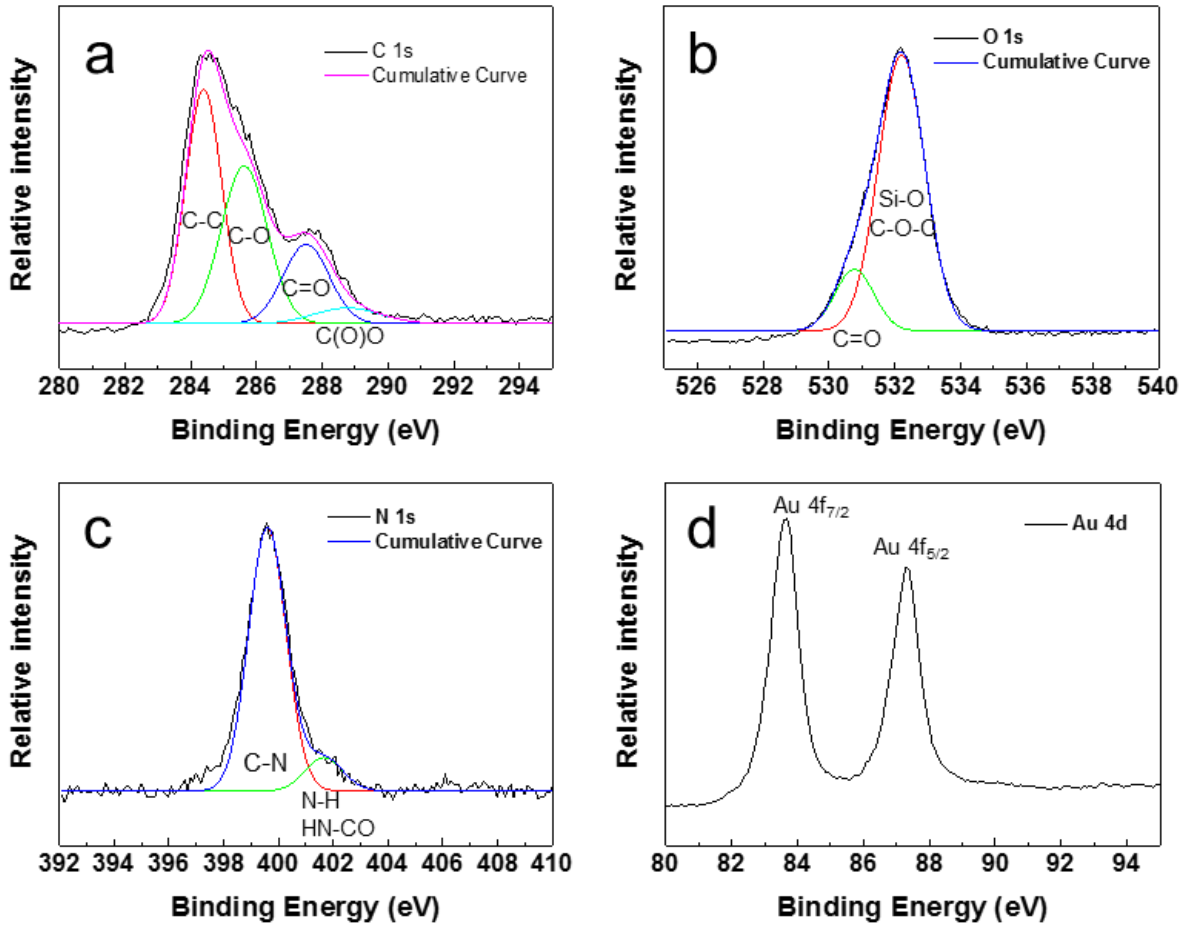

Figure 3.5 XPS spectra of Au-Den/rGO.

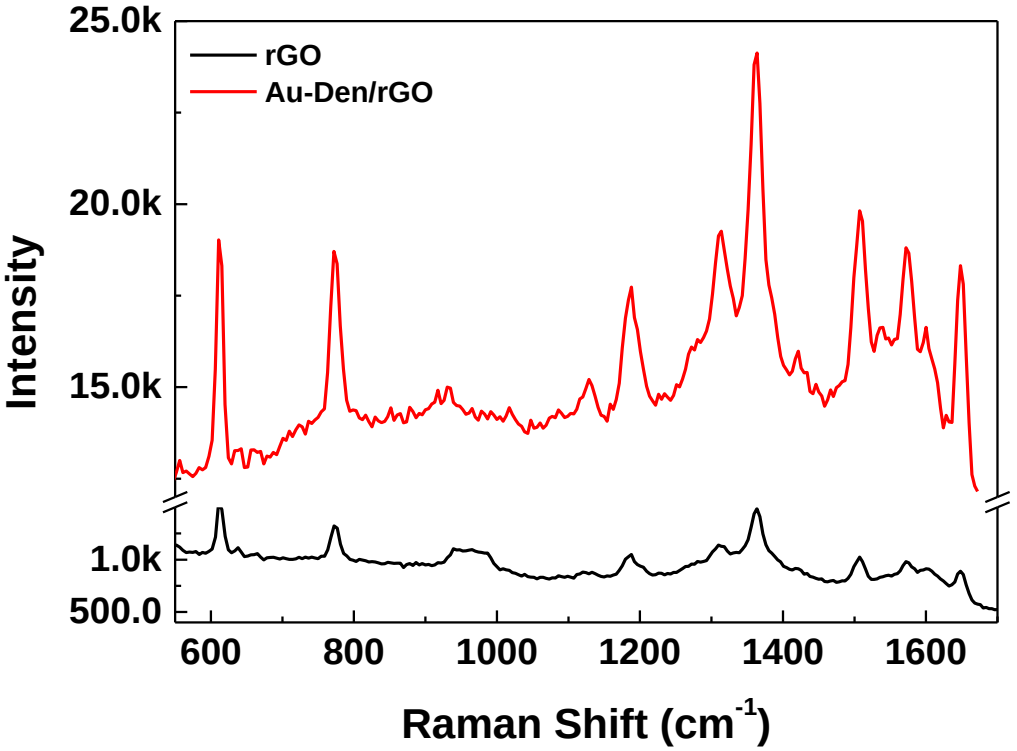

Figure 3.6 GERS of R6G on rGO/SiO_2/Si (black) and SERS of R6G on Au-Den/rGO (red) on the SiO_2/Si wafer.

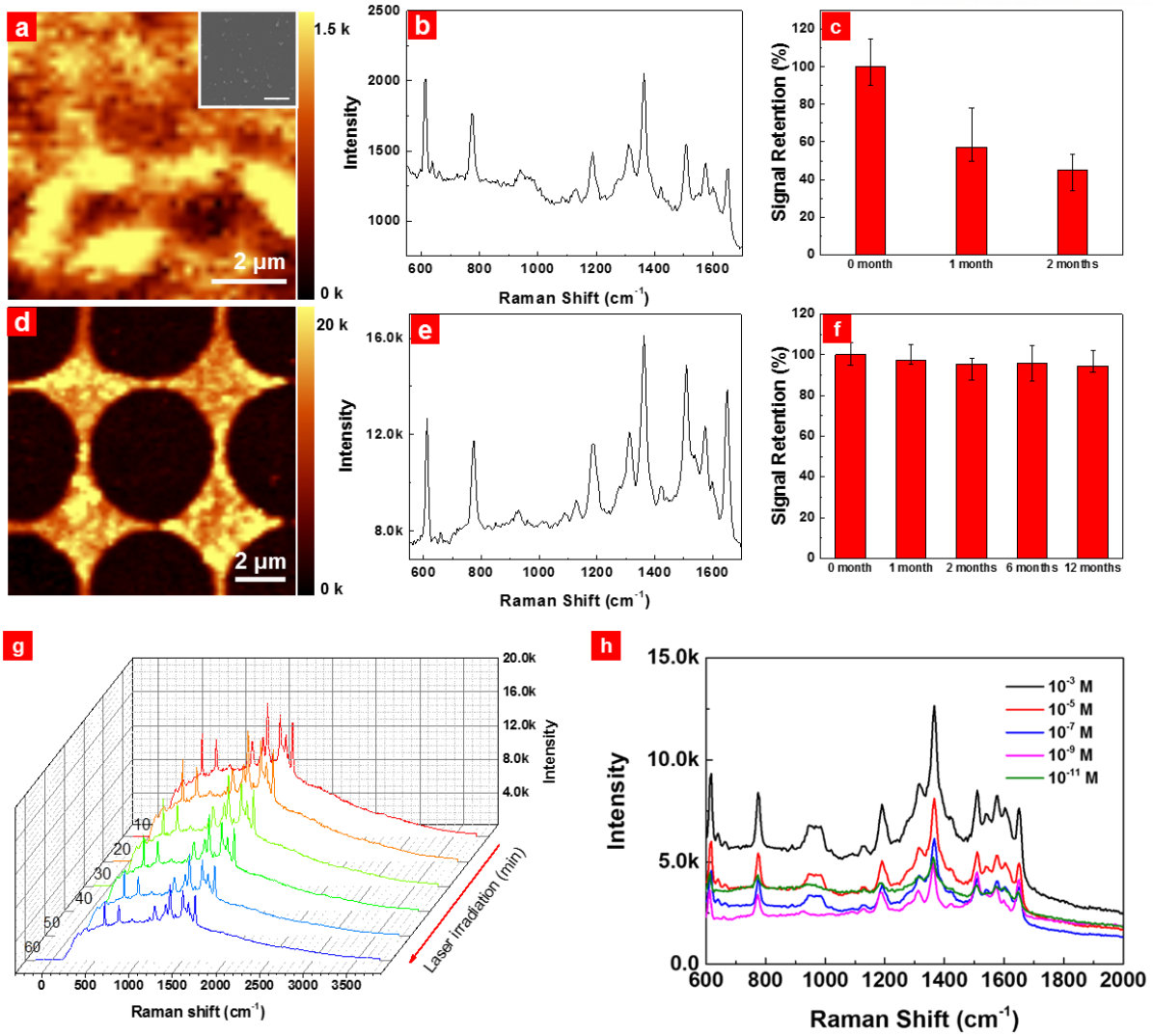

Figure 3.7 (a, d) Raman spectra of AuNPs and Au-Den/prGO. (b, e) Raman mapping data at 1370 cm^{-1} of AuNPs and Au-Den/prGO. The inset image in (b) is a SEM image of irregularly deposited AuNPs on the SiO_2 substrate. (The scale bar is 300 nm). (c, f) Histogram of Raman signal retention of R6G dyes on the AuNPs and Au-Den/prGO SERS substrate. (g) SERS stability of Au-Den/prGO with the exposure time up to 60 min. (10 min interval, 0.2 mW laser power) (h) SERS sensitivity of Au-Den/rGO at various concentrations of the R6G solution.

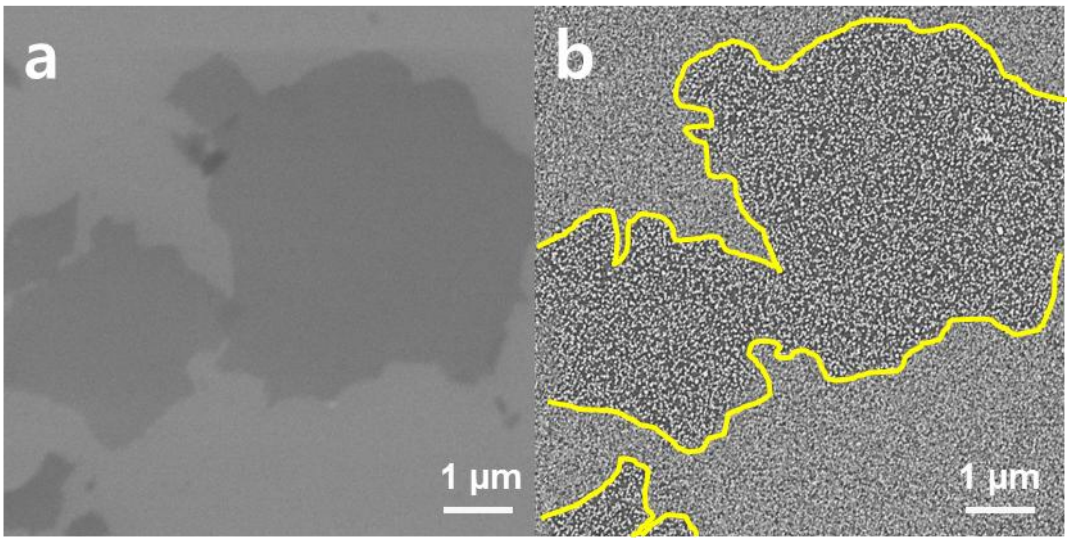

Figure 3.8 Selectivity of Au-Den on a barely coated rGO substrate. (a: before Au-Den deposition, b: after Au-Den deposition)

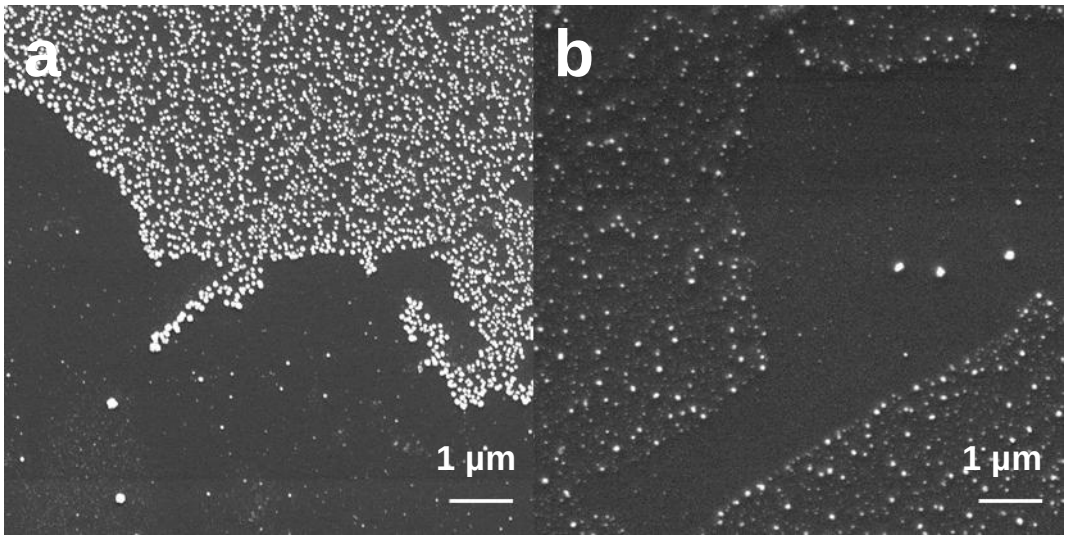

Figure 3.9 SEM image of Au-Den/prGO with different sizes of Au-Den. (a: 50 nm, b: 10 nm)

	N (mol/L)	I (cts)	τ (s)	P (mW)
Ref	10^{-5}	4000	10	20
SERS	10^{-11}	10000	10	0.2

Table 3.1 Parameters for the calculation of EF value

.

3.4 Conclusion

In summary, a facile preparation method and an optimal platform of a highly active and robust SERS substrate of Au-Den/prGO were demonstrated. The observed enhancement factor of 2.5 x 10^8 of Au-Den/prGO verified the strong SERS activity achieved by dense packing due to the strong affinity of Au-Den with rGO. The increment stems not only from the graphene and metal nanoparticles but also the synergistically combined enhancement of EM/CM in Au-Den/rGO. We also confirmed the remarkable improvement in the durability that our substrate retains its signal for more than 1 hour of laser irradiation, and that it is highly stable over one and half year. The suggested method provides a facile and straightforward way to prepare a stable and highly reliable SERS substrate for sensing biomolecules, medicine, etc. and for other real world applications.

3.5 References

1. Fleischmann, M.; Hendra, P. J.; Mcquilla.Aj, Raman-Spectra of Pyridine Adsorbed at a Silver Electrode. *Chem. Phys. Lett.* **1974,** *26* (2), 163-166.
2. Albrecht, M. G.; Creighton, J. A., Anomalously Intense Raman-Spectra of Pyridine at a Silver Electrode. *J. Am. Chem. Soc.* **1977,** *99* (15), 5215-5217.
3. Jeanmaire, D. L.; Van Duyne, R. P., Surface raman spectroelectrochemistry. *J. Electroanal. Chem. and Interfacial Electrochem.* **1977,** *84* (1), 1-20.
4. Ko, H.; Tsukruk, V. V., Nanoparticle-Decorated Nanocanals for Surface-Enhanced Raman Scattering. *Small* **2008,** *4* (11), 1980-1984.
5. Freudiger, C. W.; Min, W.; Saar, B. G.; Lu, S.; Holtom, G. R.; He, C.; Tsai, J. C.; Kang, J. X.; Xie, X. S., Label-Free Biomedical Imaging with High Sensitivity by Stimulated Raman Scattering Microscopy. *Science* **2008,** *322* (5909), 1857-1861.
6. Kundu, J.; Levin, C. S.; Halas, N. J., Real-time monitoring of lipid transfer between vesicles and hybrid bilayer on Au nanoshells using surface enhanced Raman scattering (SERS). *Nanoscale* **2009,** *1* (1), 114-117.
7. Ren, W.; Fang, Y. X.; Wang, E. K., A Binary Functional Substrate for Enrichment and Ultrasensitive SERS Spectroscopic Detection of Folic Acid Using Graphene Oxide/Ag Nanoparticle Hybrids. *ACS Nano* **2011,** *5* (8), 6425-6433.
8. Reed, J. C.; Zhu, H.; Zhu, A. Y.; Li, C.; Cubukcu, E., Graphene-Enabled Silver Nanoantenna Sensors. *Nano Lett.* **2012,** *12* (8), 4090-4094.
9. Peng, P.; Huang, H.; Hu, A. M.; Gerlich, A. P.; Zhou, Y. N., Functionalization of silver nanowire surfaces with copper oxide for surface-enhanced Raman spectroscopic bio-sensing. *J. Mater. Chem.* **2012,** *22* (31), 15495-15499.
10. Lin, D.; Qin, T.; Wang, Y.; Sun, X.; Chen, L., Graphene Oxide Wrapped SERS Tags: Multifunctional Platforms toward Optical Labeling, Photothermal Ablation of Bacteria, and the Monitoring of Killing Effect. *ACS Appl. Mater. Inter.* **2014,** *6* (2), 1320-1329.
11. Ling, X.; Xie, L.; Fang, Y.; Xu, H.; Zhang, H.; Kong, J.; Dresselhaus, M. S.; Zhang, J.; Liu, Z., Can Graphene be used as a Substrate for Raman Enhancement? *Nano Lett.* **2010,** *10* (2), 553-561.
12. Schedin, F.; Lidorikis, E.; Lombardo, A.; Kravets, V. G.; Geim, A. K.; Grigorenko, A. N.; Novoselov, K. S.; Ferrari, A. C., Surface-Enhanced Raman Spectroscopy of Graphene. *ACS Nano* **2010,** *4* (10), 5617-5626.
13. Ling, X.; Zhang, J., First-layer effect in graphene-enhanced Raman scattering. *Small* **2010,** *6* (18), 2020-5.
14. Xu, W. G.; Mao, N. N.; Zhang, J., Graphene: A Platform for Surface-Enhanced Raman Spectroscopy. *Small* **2013,** *9* (8), 1206-1224.
15. Ling, X.; Huang, S.; Deng, S.; Mao, N.; Kong, J.; Dresselhaus, M. S.; Zhang, J., Lighting Up the Raman Signal of Molecules in the Vicinity of Graphene Related Materials. *Acc. Chem. Res.* **2015**.
16. Huh, S.; Park, J.; Kim, Y. S.; Kim, K. S.; Hong, B. H.; Nam, J. M., UV/Ozone-Oxidized Large-Scale Graphene Platform with Large Chemical Enhancement in Surface-Enhanced Raman Scattering. *ACS Nano* **2011,** *5* (12), 9799-9806.
17. Yu, X. X.; Cai, H. B.; Zhang, W. H.; Li, X. J.; Pan, N.; Luo, Y.; Wang, X. P.; Hou, J. G., Tuning Chemical Enhancement of SERS by Controlling the Chemical Reduction of Graphene Oxide Nanosheets. *ACS Nano* **2011,** *5* (2), 952-958.
18. Kim, J.; Cote, L. J.; Kim, F.; Huang, J. X., Visualizing Graphene Based Sheets by Fluorescence Quenching Microscopy. *J. Am. Chem. Soc.* **2010,** *132* (1), 260-267.
19. Yang, H.; Hu, H.; Ni, Z.; Poh, C. K.; Cong, C.; Lin, J.; Yu, T., Comparison of surface-enhanced Raman scattering on graphene oxide, reduced graphene oxide and graphene surfaces. *Carbon* **2013,** *62*, 422-429.
20. Ahn, H. J.; Thiyagarajan, P.; Jia, L.; Kim, S. I.; Yoon, J. C.; Thomas, E. L.; Jang, J. H., An optimal substrate design for SERS: dual-scale diamond-shaped gold nano-structures fabricated via interference lithography. *Nanoscale* **2013,** *5* (5), 1836-42.
21. Lee, J.; Hua, B.; Park, S.; Ha, M.; Lee, Y.; Fan, Z.; Ko, H., Tailoring surface plasmons of

high-density gold nanostar assemblies on metal films for surface-enhanced Raman spectroscopy. *Nanoscale* **2014,** *6* (1), 616-23.
22. Mao, S.; Lu, G.; Yu, K.; Bo, Z.; Chen, J., Specific protein detection using thermally reduced graphene oxide sheet decorated with gold nanoparticle-antibody conjugates. *Adv. Mater.* **2010,** *22* (32), 3521-6.
23. Zhang, P.; Huang, Y.; Lu, X.; Zhang, S.; Li, J.; Wei, G.; Su, Z., One-step synthesis of large-scale graphene film doped with gold nanoparticles at liquid-air interface for electrochemistry and Raman detection applications. *Langmuir* **2014,** *30* (29), 8980-9.
24. Kim, Y. G.; Oh, S. K.; Crooks, R. M., Preparation and characterization of 1-2 nm dendrimer-encapsulated gold nanoparticles having very narrow size distributions. *Chem. Mater.* **2004,** *16* (1), 167-172.
25. Fu, Q.; Zhan, Z.; Dou, J.; Zheng, X.; Xu, R.; Wu, M.; Lei, Y., Highly Reproducible and Sensitive SERS Substrates with Ag Inter-Nanoparticle Gaps of 5 nm Fabricated by Ultrathin Aluminum Mask Technique. *ACS. Appl. Mater. Inter.* **2015,** *7* (24), 13322-8.
26. Jansen, J. F. G. A.; Debrabandervandenberg, E. M. M.; Meijer, E. W., Encapsulation of Guest Molecules into a Dendritic Box. *Science* **1994,** *266* (5188), 1226-1229.
27. Yoon, S.; In, I., Solubilization of Reduced Graphene in Water through Noncovalent Interaction with Dendrimers. *Chem. Lett.* **2010,** *39* (11), 1160-1161.
28. Herrero, M. A.; Guerra, J.; Myers, V. S.; Gomez, M. V.; Crooks, R. M.; Prato, M., Gold Dendrimer Encapsulated Nanoparticles as Labeling Agents for Multiwalled Carbon Nanotubes. *Acs Nano* **2010,** *4* (2), 905-912.
29. Kim, J. M.; Kim, J.; Kim, J., Covalent decoration of graphene oxide with dendrimer-encapsulated nanoparticles for universal attachment of multiple nanoparticles on chemically converted graphene. *Chem. Commun.* **2012,** *48* (74), 9233-5.
30. Vasumathi, V.; Pramanik, D.; Sood, A. K.; Maiti, P. K., Structure of a carbon nanotube-dendrimer composite. *Soft Matter* **2013,** *9* (4), 1372-1380.
31. Suzuki, M.; Niidome, Y.; Kuwahara, Y.; Terasaki, N.; Inoue, K.; Yamada, S., Surface-enhanced nonresonance Raman scattering from size- and morphology-controlled gold nanoparticle films. *J Phys Chem B* **2004,** *108* (31), 11660-11665.
32. Mir-Simon, B.; Reche-Perez, I.; Guerrini, L.; Pazos-Perez, N.; Alvarez-Puebla, R. A., Universal One-Pot and Scalable Synthesis of SERS Encoded Nanoparticles. *Chem. Mater.* **2015,** *27* (3), 950-958.
33. Kravets, V. G.; Jalil, R.; Kim, Y. J.; Ansell, D.; Aznakayeva, D. E.; Thackray, B.; Britnell, L.; Belle, B. D.; Withers, F.; Radko, I. P.; Han, Z.; Bozhevolnyi, S. I.; Novoselov, K. S.; Geim, A. K.; Grigorenko, A. N., Graphene-protected copper and silver plasmonics. *Sci. Rep.* **2014,** *4*, 5517.

Thanks to

우선, 이 자리에 오기까지 많은 도움을 주신 장지현 교수님께 감사드립니다. 여러가지 실망도 많이 시켜드렸지만 그럼에도 신경 쓰고 챙겨주시는 어머니의 마음에 제대로 부응하지 못해 죄송한 마음뿐입니다. 그리고 학부시절부터 저의 연구에 있어서 아버지 같은 분이자 제 인생의 전환점을 만들어주신 충주대학교 인인식 교수님께도 감사의 말씀 드리며 제가 이 자리에 오기까지 홀로 저의 뒷바라지와 지원을 아끼지 않은 어머님께도 이 자리를 빌어 감사를 전하고 싶습니다. 저의 부족한 연구실 생활을 도와준 실험실 식구들, 특히 기용이형과 익희형, 성욱이형 등 형으로써 저를 이끌어준 사람들에게 감사하고 제 고민을 들어주고 이야기해준 선이누나, 많은 고민 함께 나누었던 광현이, 짧은 시간 원하던 만큼 친해지지는 못했지만 신경 쓰고 보고 배울 수 있게 도와준 종철이형께도 감사의 말씀 전하고 싶습니다. 제가 비록 이 곳에서 연구의 길을 이어 가진 못하지만 앞으로 같은 연구선 상에 있는, 같은 배를 탄 일행으로써 생각하며 계실 때 종종 찾아 뵙고 계속해서 연락 이어갔으면 좋겠습니다. 유니스트에 있으면서 아쉬웠던 부분은 학부가 다르다 보니 후배들과 친해질 경험이 부족했는데 그런 점에서 실험 수업 조교를 하며 알게 된 후배들도 조금은 각별한 마음이 듭니다.

2008년 대학 입학 후 졸업할 때의 저 역시 느꼈던 부분이지만, 2013년 울산에 올 때의 저와, 울산을 떠나는 저의 모습이 많이 변한 것을 느낍니다. 제 고등학교 시절 교훈이 최고, 최선, 최대인데 말도 많고 탈도 많았던, 저의 석사 생활을 마무리할 수 있게 해준 많은 분들께 감사하며 앞으로도 최고의 자리에서 최선을 다한 모습으로 만나서 최대의 행복을 함께 나누고 싶습니다.